

## Orthotropic magneto-thermoelastic solid with multi-dual-phase-lag model and hall current

Parveen Lata<sup>a</sup> and Himanshi\*

*Department of Basic and Applied Sciences, Punjabi University Patiala, Punjab, India*

*(Received June 3, 2020, Revised September 15, 2020, Accepted January 26, 2021)*

**Abstract.** The present research deals with the investigation of the effect of hall current in an orthotropic magneto-thermoelastic medium with two temperature in the context of multi-phase-lag heat transfer due to thermomechanical sources. The bounding surface is subjected to linearly distributed and concentrated loads (mechanical and thermal source). Laplace and Fourier transform techniques are used to solve the problem. The expressions for displacement components, stress components and conductive temperature are derived in transformed domain and further in physical domain with the help of numerical inversion techniques. The effect of rotation and hall parameter has shown with the help of graphs.

**Keywords:** orthotropic; hall current; rotation; multi-dual-phase-lag; two temperature; laplace transform; fourier transform; concentrated and linearly distributed loads

---

### 1. Introduction

During the past few years a lot of attention has been given to the generalized theories of thermoelasticity, which admits finite speed of propagation of heat signals rather than the old thermoelasticity theories based on the classical Fourier law. These theories of generalized thermoelasticity are more realistic and appropriate than the conventional old theories. A material body deforms due to the action of external forces acting on it or due to exchange of heat with the surroundings. Temperature change results in thermal effects on materials like thermal stress, strain and deformation. When an external load is applied to a material body the mechanical waves are produced through thermal expansion. The interaction between the external applied magnetic field and the thermoelastic deformations give rise to the coupled field of magneto-thermoelasticity. The effect of magnetic field on elastic media under thermal loadings attracted several researchers due to its various applications like in electrical power engineering, in nuclear devices, optics, plasma physics, propagation of different types of waves under the influence of magnetic field, in study about the earth's rotation, moon and other planets where magnetic field experiences. The study of interaction between mechanical and thermal fields is one of the most extensive and productive area of continuum dynamics. The present model is helpful for finding the type of interaction between mechanical and thermal forces, as most of the structural elements of heavy industries are frequently

---

\*Corresponding author, Ph.D. Scholar, E-mail: [heena.zakhmi@gmail.com](mailto:heena.zakhmi@gmail.com)

<sup>a</sup>Associate Professor, E-mail: [parveenlata@pbi.ac.in](mailto:parveenlata@pbi.ac.in)

related to mechanical and thermal stresses at a higher temperature. Chen and Gurtin (1968), Chen *et al.* (1968) and Chen *et al.* (1969) formulated a theory of two temperature thermoelasticity for deformable bodies which shows that heat conduction equation depends upon two different temperatures the conductive temperature ( $\phi$ ) and the thermodynamical temperature ( $T$ ). The difference between these two temperatures is proportional to the heat supply. For time independent problems the two temperatures are same in the absence of heat supply. For time dependent problems, the two temperatures are different regardless of the presence of heat supply. Marin (1994) developed Lagrange's identity method in microstructural thermoelastic bodies. Marin (1995) proved existence and uniqueness theorem in thermoelasticity for micropolar bodies. Marin (1997) proved uniqueness of solutions of initial-boundary value problem in thermoelasticity for bodies with voids. Youssef (2006) formulated a new theory of generalized thermoelasticity by taking into account two-temperature generalized thermoelasticity theory for a homogeneous isotropic body without energy dissipation. Abbas and Youssef (2009) studied the problem of finite element analysis of two-temperature generalized magneto-thermoelasticity. Marin (2010) examined the vibrations in dipolar thermoelastic bodies. Othman *et al.* (2011) studied the effect of rotation on propagation of plane waves in fiber-reinforced thermoelastic half space using finite element method. Abbas *et al.* (2011) studied the propagation of plane waves in a fiber-reinforced anisotropic thermoelastic half space under the effect of magnetic field. Abd-alla and Abbas (2011) solved a two dimensional problem of an elastic cylinder of infinite length in the presence of constant magnetic field. Zakaria (2012) studied the effect of hall current and rotation on magneto- micropolar generalized thermoelasticity due to ramp-type heating. Kumar and Abbas (2013) studied a two dimensional problem of micropolar thermoelastic material with two temperature in the context of Lord- Shulman theory. Sharma and Marin (2014) studied the reflection and transmission of waves from imperfect boundary between two heat conducting micropolar thermoelastic solids. Abbas (2014) analyzed nonlinear transient thermal stress in a thick walled FGM cylinder. Ezzat *et al.* (2014) constructed the two temperature magneto-thermoelastic theory by using fractional order heat conduction equation. Sharma *et al.* (2015) studied the effect of inclined load in transversely isotropic thermoelastic medium with two-temperature and without energy dissipation. Das and Lahiri (2015) presented the theory of generalized magneto-thermo-elasticity to a 2D problem of a conducting thick plate under the heat source and magnetic and electric intensities. Marin *et al.* (2016) studied the mixed initial-boundary value problems for micropolar porous bodies. Kumar *et al.* (2016) studied effect of rotation in transversely isotropic magneto-thermoelastic medium with two- temperature, vacuum and with and without energy dissipation. Biswas *et al.* (2017a) studied the effect of thermal shock in magneto-thermoelastic orthotropic medium with the help of three phase lags theory. Kumar *et al.* (2017a) studied the effect of hall current and two temperatures in a transversely isotropic magneto-thermoelastic with and without energy dissipation due to ramp type heat. Biswas *et al.* (2017b) studied the propagation of Rayleigh waves in a homogeneous orthotropic thermoelastic half-space in the context of three-phase-lag model of thermoelasticity. Kumar *et al.* (2017b) investigated the Rayleigh waves in a homogeneous transversely isotropic magneto-thermoelastic in the presence of two temperature, hall current and rotation. Abbas (2018a, 2018b) studied the fractional order theory in thermoelastic half-space under thermal loading and free vibrations of nano-scale beam under two-temperature Green-Naghdi model. Lata and Kaur (2018) studied the effect of hall current in transversely isotropic magneto thermoelastic rotating medium with fractional order heat transfer due to normal force. Biswas and Abo-Dahab (2018) studied the effect of phase lags on Rayleigh wave propagation in initially stressed magneto- thermoelastic orthotropic medium. Lata (2018) studied the effect of energy dissipation on plane waves in sandwiched layered thermoelastic medium of

uniform thickness, with combined effects of two temperature, rotation and Hall current in the context of GN Type-II and Type-III theory of thermoelasticity. Lata and Kaur (2019a, 2019b, 2019c) studied various thermoelastic problems in transversely isotropic thermoelastic medium. Lata and Zakhmi (2019) studied the effect of fractional order in homogeneous orthotropic thermoelastic medium due to thermomechanical sources. Riaz et. al. (2019) studied the effect of heat and mass transfer in the Eyring power model of fluid which is propagating through a rectangular compliant channel. Bhatti et al. (2019) studied the effect of hall current and heat on the sinusoidal motion of solid particles. Abualnour et al. (2019) studied the thermomechanical analysis of antisymmetric laminated reinforced composite plates using a new four variable trigonometric refined plate theory. Belbachir et al. (2019) studied the bending analysis of anti-symmetric cross-ply laminated plates under nonlinear thermal and mechanical loadings. Draiche et al. (2019) predicted the Static analysis of laminated reinforced composite plates using a simple first-order shear deformation theory. Matouk et al. (2020) investigated the free vibrational behavior of the FG nano-beams integrated in the hygro-thermal environment and reposed on the elastic foundation by using a novel integral Timoshenko beam theory (ITBT). Chikr et al. (2020) studied a novel four- unknown integral model for buckling response of FG sandwich plates resting on elastic foundations under various boundary conditions using Galerkin's approach. Refrafi et al. (2020) analyzed the effects of hygro-thermo-mechanical conditions on the buckling of FG sandwich plates resting on elastic foundations. Rahmani et al. (2020) studied the effect of boundary conditions on the bending and free vibration behavior of FGM sandwich plates using a four-unknown refined integral plate theory.

Zenkour (2020) studied Magneto-thermal shock problem of a fiber-reinforced anisotropic half-space by using refined multi-dual-phase-lag model. Bousahla et al. (2020) investigated buckling and dynamic behavior of the simply supported CNT-RC beams using an integral-first shear deformation theory. Kaddari et al. (2020) studied the structural behaviour of functionally graded porous plates on elastic foundation using a new quasi-3D model. Tounsi et al. (2020) studied the static behavior of advanced functionally graded (AFG) ceramic-metal plates supported by a two-parameter elastic foundation and subjected to a nonlinear hygro-thermo-mechanical load. Alzahrani and Abbas (2020) studied the photo-thermal interactions in a semiconducting medium with spherical cavity and two-temperature. Lata and Zakhmi (2020) studied the orthotropic thermoelastic problem of generalized thermoelasticity with fractional order heat transfer due to time harmonic sources.

In spite of this a lot of research has been done in the area of thermoelasticity, but not much work has been done in an orthotropic magneto-thermoelastic medium with combined effects of rotation, hall current and two temperatures. Most of the large and solid bodies like earth and moon have a property of rotation with some angular velocity, so in this attempt we study the effect of rotation and hall current in two dimensional homogeneous magneto-thermoelastic orthotropic medium with two temperature in the context of multi-dual-phase-lag of generalized thermoelasticity. The effect of hall current and rotation has been examined on displacement components, stress components and conductive temperature with the help of graphs.

## 2. Basic equations

Following Chawla and Kumar (2014) the constitutive relations and basic governing equations for anisotropic thermoelastic model in the absence of body forces and heat sources are the following

$$\sigma_{ij} = c_{ijkl} e_{kl} - \beta_{ij} T, \quad (1)$$

Equation of motion as described by Schoenberg and Censor (1973) for a thermoelastic medium rotating uniformly with an angular velocity  $\boldsymbol{\Omega} = \Omega \mathbf{n}$ , where  $\mathbf{n}$  is a unit vector representing the direction of axis of rotation and taking into account Lorentz force is given as

$$\sigma_{ij,j} + F_i = \rho [\dot{u}_i + (\boldsymbol{\Omega} \times (\boldsymbol{\Omega} \times \vec{u}))_i + (2 \boldsymbol{\Omega} \times \dot{\vec{u}})_i] \quad (2)$$

$$\text{Here } F_i = \mu_0 (\vec{J} \times \vec{H}_0)_i \text{ are the components of Lorentz force} \quad (3)$$

The above equations are supplemented by generalized Ohm's law for media with finite conductivity and including the Hall current effect

$$\mathbf{J} = \frac{\sigma_0}{1+m^2} [\mathbf{E} + \mu_0 (\dot{\mathbf{u}} \times \mathbf{H} - \frac{1}{en_e} \mathbf{J} \times \mathbf{H}_0)], \quad (4)$$

Following Zenkour (2020) and Youssef (2006), the heat conduction equation with two temperature and multi-dual-phase lag is given by

$$K_{ij} \mathcal{L}_\theta \nabla^2 \phi_{ij} = \mathcal{L}_q \frac{\partial}{\partial t} [\rho C_E T + \beta_{ij} T_0 u_{i,j}], \quad (5)$$

Where  $\beta_{ij} = C_{ijkl} \alpha_{ij}$ ,  $\beta_{ij} = \beta_i \delta_{ij}$ ,  $K_{ij} = K_i \delta_{ij}$ , ( $i, j = 1, 2, 3$ );  $i$  is not summed and  $\delta_{ij}$  is Kronecker delta.

$$\mathcal{L}_\theta = 1 + \sum_{r=1}^{R_1} \frac{\tau_\theta^r}{r!} \frac{\partial^r}{\partial t^r}, \quad \mathcal{L}_q = \varrho + \tau_0 \frac{\partial}{\partial t} + \sum_{r=2}^{R_2} \frac{\tau_q^r}{r!} \frac{\partial^r}{\partial t^r}, \quad (6)$$

Generally, the value of  $R_1 = R_2 = R$  may be reach 5 or more according to refined multi-dual-phase-lag (RPL) theory required while  $\varrho$  is a non-dimension parameter ( $= 0$  or  $1$  according to the thermoelasticity theory).  $\mathcal{L}_\theta$  and  $\mathcal{L}_q$  are the two-time differential parameters in which  $\tau_q$  and  $\tau_t$  are the phase lag of the heat flux and phase lag of the temperature gradient respectively.

The strain displacement relations are

$$e_{ij} = \frac{1}{2} (u_{i,j} + u_{j,i}), \quad i, j = 1, 2, 3. \quad (7)$$

Following Youssef (2006) the two temperature relation is taken as

$$T = \phi - a_{ij} \phi_{,ij}, \quad (8)$$

Here, in all the above equations dot ( $\dot{\cdot}$ ) represents the partial derivative w.r.t time and ( $\cdot$ ) denote the partial derivative w.r.t spatial coordinate,  $c_{ijkl} (= c_{kmi j} = c_{jikm} = c_{ijmk})$  is the tensor of elastic constant,  $\rho$  is the density,  $T_0$  is the reference temperature such that  $|\frac{T}{T_0}| \ll 1$ ,  $u_i$  are the components of displacement vector  $\mathbf{u}$ ,  $C_E$  is the specific heat at constant strain,  $F_i$  are the components of Lorentz force,  $\sigma_{ij} = (\sigma_{ji})$  and are the components of stress tensor.  $T$  is the absolute temperature,  $\phi$  is the conductive temperature,  $\beta_{ij}$  are tensor of thermal moduli,  $K_{ij}$  are the components of thermal conductivity.  $\mathbf{H}$  is the magnetic strength,  $\mathbf{J}$  is the current density vector,  $\mathbf{E}$  is the intensity vector of electric field,  $m$  is the hall parameter given by  $m = \omega_e t_e = \frac{\sigma_0 \mu_0 H_0}{en_e}$  where  $t_e$  is the electron collision time where  $\omega_e = \frac{e \mu_0 H_0}{m_e}$  is the electron frequency,  $\sigma_0 = \frac{e^2 t_e n_e}{m_e}$  is the electrical conductivity,  $e$  is the charge on electron,  $m_e$  is the mass of electron and  $n_e$  is the no of density of electrons.

Following Chawla and Kumar (2014) the stress strain relations for an orthotropic medium are

given by

$$\sigma_{11} = C_{11} e_{11} + C_{13} e_{33} - \beta_1 T, \quad (9)$$

$$\sigma_{33} = C_{13} e_{11} + C_{33} e_{33} - \beta_3 T, \quad (10)$$

$$\sigma_{13} = 2 C_{55} e_{13}, \quad (11)$$

Where  $e_{11} = \frac{\partial u}{\partial x}$ ,  $e_{33} = \frac{\partial w}{\partial z}$ ,  $e_{13} = \frac{1}{2} \left( \frac{\partial u}{\partial z} + \frac{\partial w}{\partial x} \right)$ ,

and

$$T = \phi - \left( a_1 \frac{\partial^2 \phi}{\partial x^2} + a_3 \frac{\partial^2 \phi}{\partial z^2} \right). \quad (12)$$

### 3. Formulation of the problem

We consider a two dimensional perfectly conducting homogeneous orthotropic-magneto-thermoelastic medium which is rotating with an angular velocity  $\Omega = \Omega n$  initially at uniform temperature  $T_0$  with two temperature in the context of refined multi-dual-phase-lag-model with an initial magnetic field  $\vec{H} = (0, H_0, 0)$  acting in the y-axis direction. The rectangular coordinate axis  $(x, y, z)$  with z-axis pointing vertically downwards into the medium is introduced. The surface of the half-space is subjected to thermomechanical sources. For two dimensional problem in  $xz$ -plane, the components of displacement vector  $u, v$  and  $w$  and the conductive temperature  $\phi$  have the form

$$u = u(x, z, t), v = 0, w = w(x, z, t), \text{ and } \phi = \phi(x, z, t), \quad (13)$$

Let us assume that

$$\mathbf{E} = 0, \quad \Omega = (0, \Omega, 0), \quad (14)$$

The generalized ohm's law

$$J_2 = 0, \quad (15)$$

And the current density components by using eq (4) is given by

$$J_1 = \frac{\sigma_0 \mu_0 H_0}{1+m^2} \left( m \frac{\partial u}{\partial t} - \frac{\partial w}{\partial t} \right), \quad (16)$$

$$J_3 = \frac{\sigma_0 \mu_0 H_0}{1+m^2} \left( \frac{\partial u}{\partial t} + m \frac{\partial w}{\partial t} \right), \quad (17)$$

Eqs. (2) and (5) with the aid of (1), (4), (9)-(12) and (13)-(17) reduce to the form

$$\begin{aligned} C_{11} \frac{\partial^2 u}{\partial x^2} + C_{55} \frac{\partial^2 u}{\partial z^2} + (C_{13} + C_{55}) \frac{\partial^2 w}{\partial x \partial z} - \beta_1 \frac{\partial}{\partial x} \left\{ \phi - \left( a_1 \frac{\partial^2 \phi}{\partial x^2} + a_3 \frac{\partial^2 \phi}{\partial z^2} \right) \right\} - \mu_0 j_3 H_0 \\ = \rho \left( \frac{\partial^2 u}{\partial t^2} - \Omega^2 u + 2\Omega \frac{\partial w}{\partial t} \right), \end{aligned} \quad (18)$$

$$\begin{aligned} (C_{13} + C_{55}) \frac{\partial^2 u}{\partial x \partial z} + C_{55} \frac{\partial^2 w}{\partial x^2} + C_{33} \frac{\partial^2 w}{\partial z^2} - \beta_3 \frac{\partial}{\partial z} \left\{ \phi - \left( a_1 \frac{\partial^2 \phi}{\partial x^2} + a_3 \frac{\partial^2 \phi}{\partial z^2} \right) \right\} + \mu_0 j_1 H_0 \\ = \rho \left( \frac{\partial^2 w}{\partial t^2} - \Omega^2 w - 2\Omega \frac{\partial u}{\partial t} \right), \end{aligned} \quad (19)$$

$$\mathcal{L}_\theta \left( K_1 \frac{\partial^2 \phi}{\partial x^2} + K_3 \frac{\partial^2 \phi}{\partial z^2} \right) = \mathcal{L}_q \frac{\partial}{\partial t} \left[ T_0 \left( \beta_1 \frac{\partial u}{\partial x} + \beta_3 \frac{\partial w}{\partial z} \right) + \rho C_E T \right], \quad (20)$$

To facilitate the solution the following dimensionless quantities are used:-

$$\begin{aligned} x' &= \frac{x}{L}, \quad z' = \frac{z}{L}, \quad u' = \frac{\rho c_1^2}{LT_0\beta_1} u, \quad w' = \frac{\rho c_1^2}{LT_0\beta_1} w, \quad t' = \frac{c_1}{L} t, \quad \sigma'_{33} = \frac{\sigma_{33}}{T_0\beta_1}, \\ \sigma'_{31} &= \frac{\sigma_{31}}{T_0\beta_1}, \quad T' = \frac{T}{T_0}, \quad a_1' = \frac{a_1}{L}, \quad a_3' = \frac{a_3}{L}, \quad \Omega' = \frac{L}{c_1} \Omega, \quad \phi' = \frac{\phi}{T_0}. \end{aligned} \quad (21)$$

Where  $c_1^2 = \frac{c_{11}}{\rho}$  and  $L$  is a constant of dimension of length.

Using dimensionless quantities given by (21) in Eqs. (18)-(20) and suppressing the primes for convenience yield

$$\begin{aligned} \left( \frac{\partial^2 u}{\partial x^2} + \delta_1 \frac{\partial^2 u}{\partial z^2} + \delta_2 \frac{\partial^2 u}{\partial x \partial z} \right) - M \left( \frac{\partial u}{\partial t} + m \frac{\partial w}{\partial t} \right) - \frac{\partial}{\partial x} \left\{ \phi - \left( \frac{a_1}{L} \frac{\partial^2 \phi}{\partial x^2} + \frac{a_3}{L} \frac{\partial^2 \phi}{\partial z^2} \right) \right\} \\ = \frac{\partial^2 u}{\partial t^2} - \Omega^2 u + 2\Omega \frac{\partial w}{\partial t}, \end{aligned} \quad (22)$$

$$\begin{aligned} \left( \delta_3 \frac{\partial^2 w}{\partial z^2} + \delta_1 \frac{\partial^2 w}{\partial x^2} + \delta_2 \frac{\partial^2 w}{\partial x \partial z} \right) + M \left( m \frac{\partial u}{\partial t} - \frac{\partial w}{\partial t} \right) - \varepsilon \frac{\partial}{\partial z} \left\{ \phi - \left( \frac{a_1}{L} \frac{\partial^2 \phi}{\partial x^2} + \frac{a_3}{L} \frac{\partial^2 \phi}{\partial z^2} \right) \right\} \\ = \left( \frac{\partial^2 w}{\partial t^2} - \Omega^2 w - 2\Omega \frac{\partial u}{\partial t} \right), \end{aligned} \quad (23)$$

$$\mathcal{L}_\theta \left( K_1 \frac{\partial^2 \phi}{\partial x^2} + \varepsilon_1 \frac{\partial^2 \phi}{\partial z^2} \right) = \mathcal{L}_q \varepsilon_2 \frac{\partial}{\partial t} \left( \frac{\partial u}{\partial x} + \varepsilon \frac{\partial w}{\partial z} \right) + \mathcal{L}_q \varepsilon_3 \frac{\partial}{\partial t} \left\{ \phi - \left( \frac{a_1}{L} \frac{\partial^2 \phi}{\partial x^2} + \frac{a_3}{L} \frac{\partial^2 \phi}{\partial z^2} \right) \right\}, \quad (24)$$

Where  $\delta_1 = \frac{c_{55}}{c_{11}}$ ,  $\delta_2 = \frac{c_{13} + c_{15}}{c_{11}}$ ,  $\delta_3 = \frac{c_{33}}{c_{11}}$ ,  $\varepsilon_1 = \frac{K_3}{K_1}$ ,  $\varepsilon_2 = \frac{\beta_1^2 T_0 L}{\rho C_1 K_1}$ ,  $\varepsilon_3 = \frac{\rho C_E}{K_1}$ ,  $M = \frac{\sigma_0 \mu_0^2 H_0^2 L}{\rho C_1 (1+m^2)}$ ,  $\varepsilon = \frac{\beta_3}{\beta_1}$ .

Apply Laplace and Fourier transforms defined by

$$\bar{f}(x, z, s) = \int_0^\infty f(x, z, t) e^{-st} dt, \quad (25)$$

$$\hat{f}(\xi, z, s) = \int_{-\infty}^\infty \bar{f}(x, z, s) e^{i\xi x} dx, \quad (26)$$

On Eqs. (22)-(24), we obtain a system of three homogeneous equations. These resulting equations have non-trivial solutions if the determinant of the coefficient matrix  $(\hat{u}, \hat{w}, \hat{\phi})$  vanishes, which yields

$$(PD^6 + QD^4 + RD^2 + S)(\hat{u}, \hat{w}, \hat{\phi}) = 0, \quad (27)$$

Where

$$D = \frac{d}{dz},$$

$$P = \zeta_2 \varepsilon_1 \mathcal{L}'_\theta + \mathcal{L}'_q (\varepsilon_3 s \zeta_2 \zeta_3 + \delta_2 \varepsilon_2 \varepsilon^2 \zeta_3 s),$$

$$Q = \mathcal{L}'_\theta \left( -\delta_1^2 \zeta_8 - \xi^2 \zeta_2 - \delta_1 \varepsilon_1 \zeta_7 - \delta_3 \zeta_8 - \delta_3 \varepsilon_1 \zeta_7 + \zeta_{12} \varepsilon_1 \right) + \mathcal{L}'_q \left\{ \zeta_{13} \left( -\zeta_{11} \zeta_3 - \zeta_2 \zeta_5 - \delta_1 \zeta_3 \zeta_7 - \xi^2 \zeta_3 \delta_3 - \delta_3 \zeta_3 \zeta_7 + \zeta_{12} \zeta_3 \right) - \zeta_{14} \left( \zeta_5 \delta_2 + \xi^2 \zeta_3 + \zeta_3 \zeta_7 \right) + \xi^2 \varepsilon_2 s \zeta_3 + 2 \varepsilon (\delta_2 - \delta_3) \right\},$$

$$R = \mathcal{L}'_\theta \left\{ \xi^2 (\zeta_{11} + \delta_1 (\zeta_7 + \zeta_8)) + \delta_3 \xi^2 (\zeta_7 + \xi^2) + \zeta_7 \zeta_8 + \delta_1 \zeta_8 \zeta_7 + \zeta_6 (s + 2 \zeta_{10} - 2 \zeta_9) - \zeta_9 (2s^2 - \Omega^2) + \zeta_{10} (s^2 + \frac{\zeta_6^2}{s^2} m^2 + 4m \Omega \frac{\zeta_6}{s} + 4\Omega^2) \right\} + \mathcal{L}'_q \left\{ \zeta_{13} \zeta_5 (\zeta_{11} + \delta_1 \zeta_7) + \zeta_{13} \xi^2 \left\{ (\delta_3 \zeta_5 + \zeta_3 \zeta_7) + \delta_1 \zeta_3 (\xi^2 + s) \right\} + \zeta_{13} \delta_3 \zeta_6 \zeta_5 + \zeta_6 \zeta_{13} \zeta_3 \zeta_7 - \zeta_{13} \delta_3 \Omega^2 \zeta_5 - \zeta_{13} \Omega^2 \zeta_3 \zeta_7 - \delta_1 \xi^2 \zeta_{13} \zeta_3 (s^2 - \Omega^2) + \varepsilon_3 s^3 (\delta_3 \zeta_5 + \zeta_7) + \zeta_{14} \xi^2 \zeta_5 + \zeta_{14} \zeta_7 \zeta_5 - \zeta_{12} \zeta_{13} \zeta_5 - \delta_2 \varepsilon \varepsilon_2 s \xi^2 \zeta_5 + \zeta_6^2 \zeta_{13} m^2 \zeta_3 + 4s m \zeta_{13} \zeta_6 \Omega \zeta_3 + 4\Omega^2 s^2 \zeta_{13} \zeta_3 - \delta_2 \varepsilon \varepsilon_2 s \xi^2 \zeta_5 + \varepsilon_2 s \delta_3 \xi^2 \zeta_5 + \varepsilon_2 s \delta_1 \xi^4 \zeta_3 + \varepsilon_2 s \xi^2 \zeta_3 \zeta_7 \right\},$$

$$S = \mathcal{L}'_\theta \left\{ -\delta_1 \xi^6 - \xi^4 \zeta_7 (1 + \delta_1) - \xi^2 \zeta_7^2 - \xi^2 \zeta_6^2 m^2 - 2\xi^2 s^2 (\Omega M \cdot m + 2\Omega^2) \right\}$$

$$+\mathcal{L}'_q \{ -\delta_1 \xi^4 \zeta_{13} \zeta_5 - \xi^2 \zeta_5 \zeta_{13} \zeta_7 - \delta_1 \xi^2 \zeta_{13} \zeta_6 + 2\zeta_{13} \zeta_6 \zeta_5 \zeta_7 + \delta_1 \xi^2 \Omega^2 \zeta_{13} \zeta_5 - \delta_1 \xi^2 s^2 \zeta_{13} \zeta_5 - \zeta_5 \zeta_6 \zeta_{13} s^2 - \zeta_5 \zeta_{13} s^4 - \zeta_6^2 \zeta_{13} \zeta_5 m^2 - 4m\Omega s^2 \zeta_6 \zeta_{13} \zeta_5 - 3s^2 \Omega^2 \zeta_5 \zeta_{13} - \delta_1 \varepsilon_2 s \xi^4 \zeta_5 - \varepsilon_2 s \xi^2 \zeta_7 - \varepsilon_2 s \xi^4 \zeta_1 \zeta_7 \}.$$

Where

$$\zeta_1 = \frac{\alpha_1}{L}, \zeta_2 = \delta_1 \delta_3, \zeta_3 = \frac{\alpha_3}{L}, \zeta_4 = \varepsilon_1 \delta_3, \zeta_5 = \left(1 + \xi^2 \frac{\alpha_1}{L}\right), \zeta_6 = M' s, \zeta_7 = (s^2 + \zeta_6 - \Omega^2), \zeta_8 = \xi^2 \varepsilon_1,$$

$$\zeta_9 = \Omega^2 \varepsilon_1, \zeta_{10} = s^2 \varepsilon_1, \zeta_{11} = \xi^2 \delta_1^2, \zeta_{12} = \xi^2 \delta_2^2, \zeta_{13} = \varepsilon_3 s, \zeta_{14} = \varepsilon_2 \varepsilon^2 s,$$

$$\mathcal{L}'_\theta = \frac{1}{s} + \sum_{r=1}^{R_1} \frac{\tau_\theta^r}{r!} s^r,$$

$$\mathcal{L}'_q = \frac{\rho}{s} + \frac{\tau_0 c_1}{L} s \sum_{r=2}^{R_2} \frac{\tau_q^r}{r!} s^r.$$

The above Eq. (27) can be written as  $[(D^2 - \lambda_1^2)(D^2 - \lambda_2^2)(D^2 - \lambda_3^2)](\hat{u}, \hat{w}, \hat{\phi}) = 0,$

Where  $\pm \lambda_i (i = 1, 2, 3)$  are the roots of the Eq. (27), the solution of the equation satisfying the radiation conditions can be written as

$$\tilde{u} = A_1 e^{-\lambda_1 z} + A_2 e^{-\lambda_2 z} + A_3 e^{-\lambda_3 z}, \tag{28}$$

$$\tilde{w} = d_1 A_1 e^{-\lambda_1 z} + d_2 A_2 e^{-\lambda_2 z} + d_3 A_3 e^{-\lambda_3 z}, \tag{29}$$

$$\tilde{\phi} = l_1 A_1 e^{-\lambda_1 z} + l_2 A_2 e^{-\lambda_2 z} + l_3 A_3 e^{-\lambda_3 z}, \tag{30}$$

Where

$$d_i = \frac{\lambda_i^4 A^* + \lambda_i^2 B^* + C^*}{\lambda_i^4 A' + \lambda_i^2 B' + C'}; i = 1, 2, 3 \tag{31}$$

$$l_i = \frac{\lambda_i^4 P' + \lambda_i^2 Q' + R'}{\lambda_i^4 A' + \lambda_i^2 B' + C'}; i = 1, 2, 3 \tag{32}$$

Where

$$A^* = \mathcal{L}'_\theta (\delta_1 \varepsilon_1) + \mathcal{L}'_q (\delta_1 \zeta_{13} \zeta_3),$$

$$B^* = \mathcal{L}'_\theta \{ -\xi^2 (\delta_1 + \varepsilon_1) - \varepsilon_1 \zeta_7 \} + \mathcal{L}'_q \{ -\delta_1 \zeta_{13} \zeta_5 - \zeta_{13} \zeta_3 \xi^2 - \zeta_{13} \zeta_3 \zeta_7 - \zeta_3 \varepsilon_2 s \xi^2 \},$$

$$C^* = \mathcal{L}'_\theta \{ \xi^4 + \xi^2 \zeta_7 \} + \mathcal{L}'_q \{ \xi^2 \zeta_{13} \zeta_5 + \zeta_{13} \zeta_6 \zeta_5 \zeta_7 + \varepsilon_2 s \xi^2 \zeta_5 \},$$

$$A' = \{ \mathcal{L}'_\theta \zeta_4 + \mathcal{L}'_q (\zeta_3 \zeta_{14}) \},$$

$$B' = \mathcal{L}'_\theta \{ \xi^2 (-\delta_1 \varepsilon_1 - \delta_3) - \varepsilon_1 \zeta_7 \} + \mathcal{L}'_q \{ -\xi^2 \delta_1 \zeta_{13} \zeta_3 - \zeta_{13} \delta_3 \zeta_5 - \zeta_{13} \zeta_3 \zeta_7 - \zeta_{14} \zeta_5 \},$$

$$C' = \mathcal{L}'_\theta \{ \xi^4 \delta_1 + \xi^2 \zeta_7 \} + \mathcal{L}'_q \{ \xi^2 \delta_1 \zeta_{13} \zeta_5 + \zeta_{13} \delta_3 \zeta_3 + \zeta_6 \zeta_{13} \zeta_5 + \zeta_{13} \zeta_5 s^2 - \zeta_{13} \zeta_5 \Omega^2 \},$$

$$P' = \{ \delta_1 \delta_3 \},$$

$$Q' = \{ \zeta_{12} - \zeta_{11} - \delta_1 \zeta_7 - \delta_3 \xi^2 - \delta_3 \zeta_7 \},$$

$$R' = \{ \xi^2 \zeta_7 + \delta_1 \xi^4 + \delta_1 \xi^2 \zeta_7 + \zeta_6^2 + 2\zeta_6 (s^2 - \Omega^2) + s^4 + \Omega^4 + m^2 \zeta_7^2 + 4\Omega s^2 m M' + 2\Omega^2 s^2 \}.$$

#### 4. Boundary conditions

Following Kumar *et al.* (2016), we apply a normal force and thermal source on the half-space surface ( $z=0$ ). The boundary conditions are given by

$$\sigma_{33} = -F_1 \psi_1(x) \delta(t), \tag{33}$$

$$\sigma_{31} = 0, \tag{34}$$

$$\frac{\partial T}{\partial z} = F_2 \psi_2(x) \delta(t) \text{ at } z = 0. \quad (35)$$

Where  $F_1$  is the magnitude of force applied,  $F_2$  is the constant temperature applied on the boundary,  $\psi_1(x)$  and  $\psi_2(x)$  are the source distribution function along  $x$ -axis.

By applying Laplace and Fourier transform defined by (25)-(26) on the boundary conditions (33)-(35) and with the help of Eqs. (9)-(12),(21),(28)-(30), we obtain components of displacement, normal stress, tangential stress and conductive temperature as

$$\begin{aligned} \tilde{u} = & -\frac{F_1 \tilde{\psi}_1(\xi)}{\Delta} (\Delta_1 e^{-\lambda_1 z} + \Delta_2 e^{-\lambda_2 z} + \Delta_3 e^{-\lambda_3 z}) + \\ & \frac{F_2 \tilde{\psi}_2(\xi)}{\Delta} (\Delta_1^* e^{-\lambda_1 z} + \Delta_2^* e^{-\lambda_2 z} + \Delta_3^* e^{-\lambda_3 z}), \end{aligned} \quad (36)$$

$$\begin{aligned} \tilde{w} = & -\frac{F_1 \tilde{\psi}_1(\xi)}{\Delta} (d_1 \Delta_1 e^{-\lambda_1 z} + d_2 \Delta_2 e^{-\lambda_2 z} + d_3 \Delta_3 e^{-\lambda_3 z}) + \frac{F_2 \tilde{\psi}_2(\xi)}{\Delta} (d_1 \Delta_1^* e^{-\lambda_1 z} \\ & + d_2 \Delta_2^* e^{-\lambda_2 z} + d_3 \Delta_3^* e^{-\lambda_3 z}), \end{aligned} \quad (37)$$

$$\begin{aligned} \tilde{\phi} = & -\frac{F_1 \tilde{\psi}_1(\xi)}{\Delta} (l_1 \Delta_1 e^{-\lambda_1 z} + l_2 \Delta_2 e^{-\lambda_2 z} + l_3 \Delta_3 e^{-\lambda_3 z}) \\ & + \frac{F_2 \tilde{\psi}_2(\xi)}{\Delta} (l_1 \Delta_1^* e^{-\lambda_1 z} + l_2 \Delta_2^* e^{-\lambda_2 z} + l_3 \Delta_3^* e^{-\lambda_3 z}), \end{aligned} \quad (38)$$

$$\begin{aligned} \tilde{\sigma}_{33} = & -\frac{F_1 \tilde{\psi}_1(\xi)}{\Delta} (\Delta_{11} \Delta_1 e^{-\lambda_1 z} + \Delta_{12} \Delta_2 e^{-\lambda_2 z} + \Delta_{13} \Delta_3 e^{-\lambda_3 z}) \\ & + \frac{F_2 \tilde{\psi}_2(\xi)}{\Delta} (\Delta_{11} \Delta_1^* e^{-\lambda_1 z} + \Delta_{12} \Delta_2^* e^{-\lambda_2 z} + \Delta_{13} \Delta_3^* e^{-\lambda_3 z}), \end{aligned} \quad (39)$$

$$\begin{aligned} \tilde{\sigma}_{13} = & -\frac{F_1 \tilde{\psi}_1(\xi)}{\Delta} (\Delta_{21} \Delta_1 e^{-\lambda_1 z} + \Delta_{22} \Delta_2 e^{-\lambda_2 z} + \Delta_{23} \Delta_3 e^{-\lambda_3 z}) \\ & + \frac{F_2 \tilde{\psi}_2(\xi)}{\Delta} (\Delta_{21} \Delta_1^* e^{-\lambda_1 z} + \Delta_{22} \Delta_2^* e^{-\lambda_2 z} + \Delta_{23} \Delta_3^* e^{-\lambda_3 z}), \end{aligned} \quad (40)$$

Where

$$\begin{aligned} \Delta &= \Delta_{11} (\Delta_{22} \Delta_{33} - \Delta_{32} \Delta_{23}) - \Delta_{12} (\Delta_{21} \Delta_{33} - \Delta_{23} \Delta_{31}) + \Delta_{13} (\Delta_{21} \Delta_{32} - \Delta_{22} \Delta_{31}), \\ \Delta_1^* &= (\Delta_{12} \Delta_{23} - \Delta_{13} \Delta_{22}), \quad \Delta_2^* = (\Delta_{13} \Delta_{21} - \Delta_{11} \Delta_{23}), \quad \Delta_3^* = (\Delta_{11} \Delta_{22} - \Delta_{12} \Delta_{21}), \\ \Delta_{1j} &= \frac{c_{13} \xi^i}{\rho c_1^2} - \frac{c_{33} d_j \lambda_j}{\rho c_1^2} - \varepsilon l_j - \varepsilon a_1 \xi^2 l_j + \varepsilon a_3 \lambda_j^2 l_j; \quad j=1, 2, 3 \\ \Delta_{2j} &= \frac{c_{55}}{\rho c_1^2} [-\lambda_j + i \xi d_j]; \quad j=1, 2, 3. \end{aligned}$$

#### 4.1 Thermal source on the surface of half-space

Taking  $F_1=0$  in Eqs. (36)-(40), we obtain the components of tangential stress, normal stress, displacement components and conductive temperature due to thermal source.

#### 4.2 Mechanical force on the surface of half-space

Taking  $F_2=0$  in Eqs. (36)-(40), we obtain the components of tangential stress, normal stress, displacement components and conductive temperature due to mechanical force.

## 5. Applications

### 5.1 Linearly distributed force

The solution due to linearly distributed force is obtained by setting

$$\{\psi_1(x), \psi_2(x)\} = \begin{cases} 1 & \text{if } |x| \leq m \\ 0 & \text{if } |x| > m \end{cases} \quad (41)$$

In Eqs. (33) and (35). The Laplace and Fourier transforms of  $\psi_1(x)$  and  $\psi_2(x)$  with respect to the pair  $(x, \xi)$  in case of linearly distributed load of non-dimensional width  $2m$  applied at origin of co-ordinate system  $x = z = 0$  is given by

$$\{\widehat{\psi}_1(\xi), \widehat{\psi}_2(\xi)\} = [2(1 - \cos(\xi m) / \xi^2 m)], \xi \neq 0. \quad (42)$$

Using (42) in (36)-(40), we get the components of tangential stress, normal stress, tangential displacement, normal displacement, conductive temperature.

### 5.2 concentrated force

The solution due to concentrated normal force is obtained by setting

$$\psi_1(x) = \delta(x), \quad \psi_2(x) = \delta(x), \quad (43)$$

In Eqs. (33) and (35). Here  $\delta(x)$  is the Dirac delta function. By applying Laplace and Fourier transformations defined in Eqs. (21)-(22) on (43), we get

$$\widehat{\psi}_1(\xi) = 1, \quad \widehat{\psi}_2(\xi) = 1. \quad (44)$$

Using (44) in (36)-(40), we obtain the components of tangential stress, normal stress, displacement and conductive temperature.

## 6. Inversion of transformation

To obtain the solution of the problem in physical domain, we must invert the transformations in Eqs. (36)-(40). Here the displacement components, tangential and normal stresses and conductive temperature are functions of  $z$ , the parameters of Laplace and Fourier transforms  $s$  and  $\xi$  respectively and are of the form  $f(\xi, z, s)$ . To obtain the function  $f(x, z, t)$  in the physical domain, we first invert the Fourier transform using

$$\bar{f}(x, z, s) = \frac{1}{2\pi} \int_{-\infty}^{\infty} e^{i\xi x} \hat{f}(\xi, z, s) d\xi = \frac{1}{2\pi} \int_{-\infty}^{\infty} [\cos(\xi x) f_e - i \sin(\xi x) f_o] d\xi, \quad (45)$$

Where  $f_o$  and  $f_e$  are respectively the odd and even parts of  $\hat{f}(\xi, z, s)$ . Thus the expression (45) gives the Laplace transform  $\bar{f}(x, z, s)$  of the function  $f(x, z, t)$ . Following Honig and Hirdes (1984), the Laplace transform function  $\bar{f}(x, z, s)$  can be inverted to  $f(x, z, t)$ . The last step is to calculate the integral in Eq. (45). The method of evaluating this integral is described in Press *et al.* (1986). It involves the use of Romberg's integration with adaptive step size. This also uses the results from successive refinements of the extended trapezoidal rule followed by extrapolation of the results to the limit when the step size tends to zero.

## 7. Numerical results and discussion

Following Biswas *et al.* (2017b), the following values of relevant parameters for cobalt material are taken

$$c_{11}=3.071 \times 10^{11} \text{Kgm}^{-1}\text{s}^{-2}, c_{13}=1.650 \times 10^{11} \text{Kgm}^{-1}\text{s}^{-2}, a_1 = 0.05, a_3 = 0.08, \mu_0 = 1.2571 \times 10^6 \text{Hm}^{-1}, c_{33}=3.581 \times 10^{11} \text{Kgm}^{-1}\text{s}^{-2}, c_{55}=1.510 \times 10^{11} \text{Kgm}^{-1}\text{s}^{-2}, T_0=0.293 \times 10^3 \text{K}, C_E = 4.27 \times 10^2 \text{J/KgK}, \beta_1=7.04 \text{Nm}^2\text{K}^{-1}, \beta_3=6.90 \text{Nm}^2\text{K}^{-1}, \rho=8.836 \times 10^3 \text{Kgm}^{-3}, K_1=0.690 \times 10^2 \text{Wm}^{-1}\text{K}^{-1}, K_3=0.690 \times 10^2 \text{Wm}^{-1}\text{K}^{-1}, \tau_0 = 2.0 \times 10^{-7} \text{s}, \tau_\theta=1.5 \times 10^{-7} \text{s}, \tau_q = 2.0 \times 10^{-7} \text{s}, H_0 = 1 \text{Jm}^{-1}\text{nb}^{-1}, \epsilon_0 = 8.838 \times 10^{-12} \text{Fm}^{-1},$$

$$L=1, \varrho = 1.$$

Using above values of parameters, the graphical representation of components of tangential stress, normal stress, tangential and normal displacements and conductive temperature with distance 'x' has been derived for an orthotropic body by using two different values of hall parameter  $m=0.25$  and  $m=0.5$  with and without rotation i.e.,  $\Omega=4, 0$  respectively.

- (1) The red solid line with centre symbol diamond ( $\diamond$ ) for an orthotropic material corresponds to hall parameter  $m=0.25$  with  $\Omega=0$ .
- (2) The green solid line with centre symbol plus (+) for an orthotropic material corresponds to hall parameter  $m=0.25$  with  $\Omega=4$ .
- (3) The blue solid line with centre symbol circle ( $\Delta$ ) for an orthotropic material corresponds to hall parameter  $m=0.5$  with  $\Omega=0$ .
- (4) The pink solid line with centre symbol circle ( $\circ$ ) for an orthotropic material corresponds to hall parameter  $m=0.5$  with  $\Omega=4$ .

## 8. Particular cases

1. If  $\tau_\theta = \tau_q = \tau_0 = 0$  and  $\varrho=1$  in the Eq. (5), the resulting equation with two parameters  $\mathcal{L}_\theta = 1$  and  $\mathcal{L}_q=1$  represents heat equation for coupled theory of thermoelasticity (1956).
2. The heat conduction Eq. (5) for the case of Lord Shulman theory (1967) is obtained by setting  $\varrho = 1$  and  $\tau_\theta, \tau_q \rightarrow 0, \tau_0 > 0$  and  $\mathcal{L}_\theta = 1$  and  $\mathcal{L}_q=1 + \tau_0 \frac{\partial}{\partial t}$ ,
3. The heat conduction Eq. (5) reduces for the case G-N theory of type II (1993) by setting  $\tau_\theta, \tau_q \rightarrow 0, \varrho=0$  and  $\tau_0 = 1$  in Eq. (5) and  $\mathcal{L}_\theta = 1, \mathcal{L}_q=\frac{\partial}{\partial t}$ ,
4. The simplest form of the heat equation with dual-phase-lag (1995), is applied by setting  $\mathcal{L}_\theta = 1 + \tau_\theta \frac{\partial}{\partial t}, \mathcal{L}_q=1 + \tau_q \frac{\partial}{\partial t}$ , in Eq. (5).
5. Additional refined dual-phase-lag (RDPL) theory appeared in the literature (1995) is defined by including the effect of the term containing  $\tau_q^2$  in the above equations as

$$\mathcal{L}_\theta = 1 + \tau_\theta \frac{\partial}{\partial t}, \mathcal{L}_q = 1 + \tau_q \frac{\partial}{\partial t} + \tau_q^2 \frac{\partial^2}{\partial t^2}. \quad (46)$$

Above Eq. (46) represents the first type of present refined multi-dual-phase-lag (RPL) theory with  $\varrho=1, \tau_0 \rightarrow \tau_q$  and  $R_1 = 1, R_2 = 2$  additional types are presented here for  $R_1 = R_2 = R \geq 2$ .

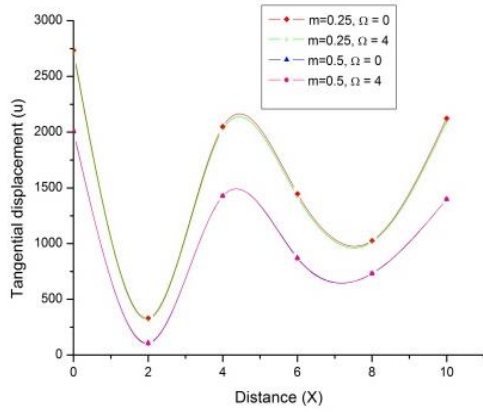


Fig. 1 Variation of displacement  $u$  with distance  $x$  (linearly distributed thermal source)

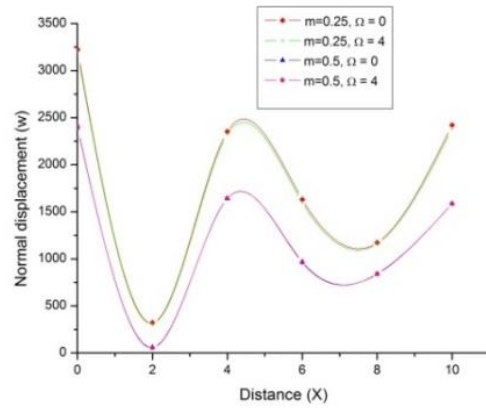


Fig. 2 Variation of normal displacement  $w$  with distance  $x$  (linearly distributed thermal source)

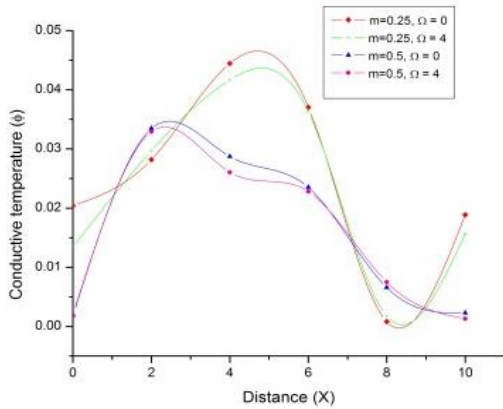


Fig. 3 Variation of conductive temperature  $\phi$  with distance  $x$  (linearly distributed thermal source)

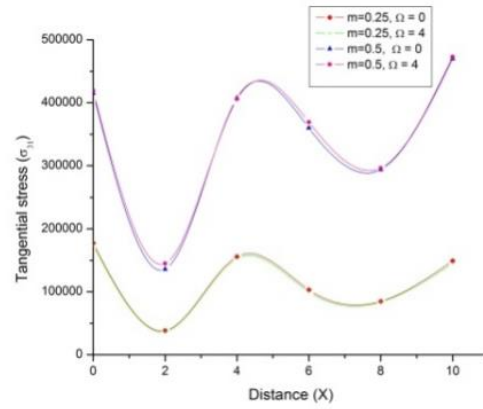


Fig. 4 Variation of tangential stress  $\sigma_{31}$  with distance  $x$  (linearly distributed thermal source)

## 9. Deformation due to thermal source

### 9.1 linearly distributed thermal source

In linearly distributed thermal source, we examined the variations of all the components with distance  $x$  for two values of hall parameter  $m=0.25$  and  $m=0.5$  with  $\Omega=0$  and  $\Omega=4$  respectively. Fig. 1 displays the variation of displacement  $u$  with distance  $x$ . We observe that for both values  $m=0.25$  and  $m=0.5$  it increases gradually then decreases. It attains a peak value in the range  $4 \leq x \leq 5$  and in the rest behaves in oscillatory manner, for  $m=0.25$  amplitude of oscillations are higher as compared to  $m=0.5$  with  $\Omega=0, 4$  respectively. Fig. 2 interprets the variation of normal displacement  $w$  with distance  $x$ . We noticed that variations are similar as in case of displacement  $u$ . It also follows an oscillatory pattern for  $m=0.25$  and  $m=0.5$  with  $\Omega=0, 4$  in the whole range with minimum and maximum amplitudes. The variation of conductive temperature  $\phi$  with distance  $x$  has shown in Fig. 3. We see that for  $m=0.25$  and  $\Omega=0, 4$  in the range  $0 \leq x \leq 4$  near the loading surface there is a

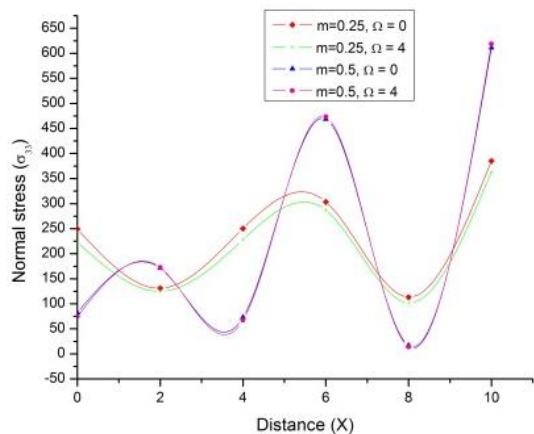


Fig. 5 Variation of normal stress  $\sigma_{33}$  with distance  $x$  (linearly distributed thermal source)

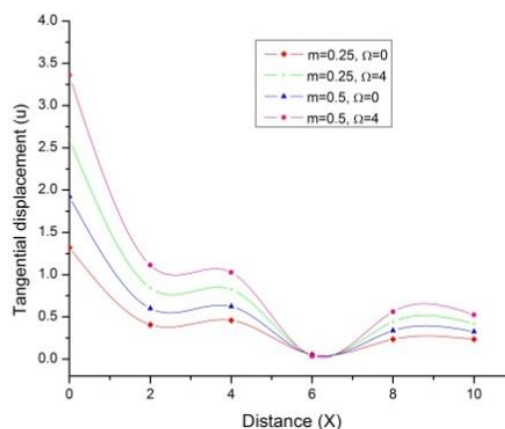


Fig. 6 Variation of displacement  $u$  with distance  $x$  (concentrated thermal source)

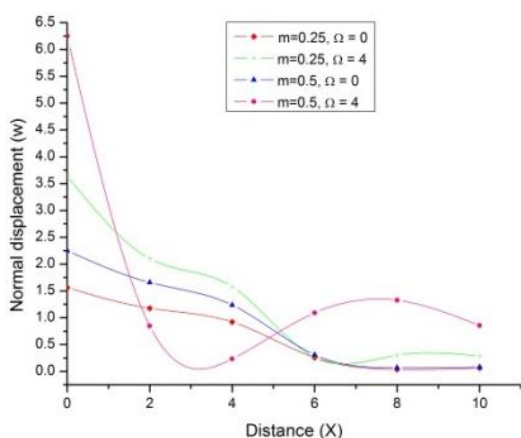


Fig. 7 Variation of normal displacement  $w$  with distance  $x$  (concentrated thermal source)

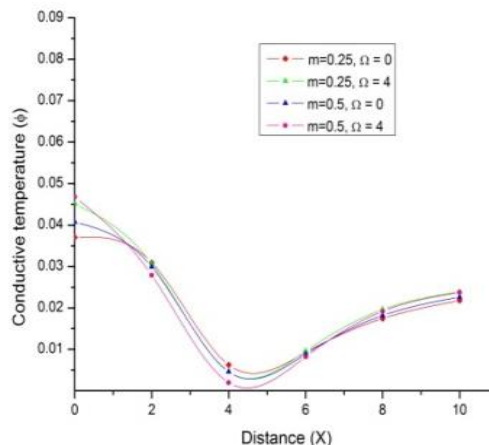


Fig. 8 Variation of conductive temperature  $\phi$  with distance (concentrated thermal source)

sharp increase with increasing value of  $x$ . It has a maximum value near  $x=5$  after that it decreases in the range  $6 \leq x \leq 8$  then a smooth increase is observed i.e., behavior is oscillatory. For  $m=0.5$  and  $\Omega=0, 4$  it varies from minimum to maximum value in the range  $0 \leq x \leq 2$  then a sudden decrease with increase in the value of  $x$ , and all the curves meet each other at  $x=9$ . Fig. 4 and Fig. 5 exhibits the trends of tangential stress  $\sigma_{31}$  and normal stress  $\sigma_{33}$  with distance  $x$ . In Fig. 4 it can be seen that the trends are similar oscillatory with difference in magnitude of oscillations, but amplitude of oscillations are higher in case of  $m=0.5$  as compared to  $m=0.25$  with  $\Omega=0, 4$  respectively. Fig. 5 describes that the value of normal stress decreases near the loading surface with  $m=0.25$  and  $\Omega=0, 4$  and increases near the loading surface with  $m=0.5$  and  $\Omega=0, 4$  i.e., it follows a smooth oscillatory pattern in the whole range of distance. It is clear from the graphs that the behavior is oscillatory with minimum and maximum amplitudes of oscillations in the whole range or we can say that rotation forces to move in oscillatory manner.

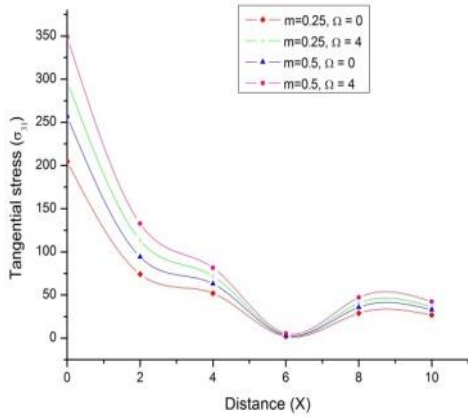


Fig. 9 Variation of tangential stress  $\sigma_{31}$  with distance  $x$  (concentrated thermal source)

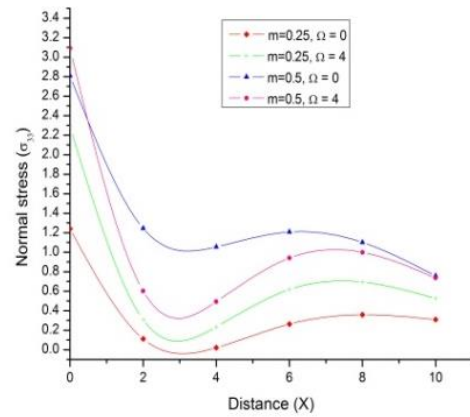


Fig. 10 Variation of Normal stress  $\sigma_{33}$  with distance  $x$  (concentrated thermal source)

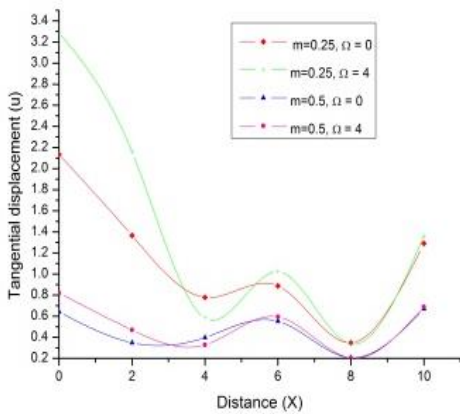


Fig. 11 Variation of displacement  $u$  with distance  $x$  (linearly distributed mechanical force)

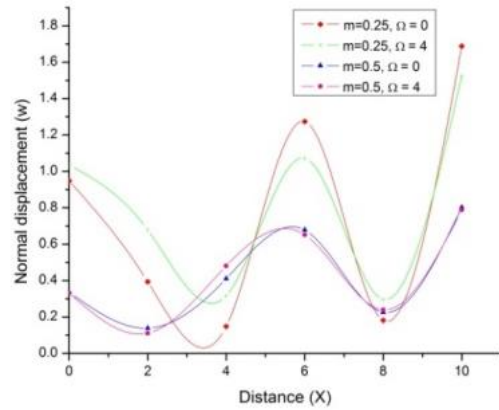


Fig. 12 Variation of normal displacement  $w$  with distance  $x$  (linearly distributed mechanical force)

### 9.2 Concentrated thermal source

In concentrated thermal source, Fig. 6 depicts the variation of displacement  $u$  with distance  $x$ . The value of displacement  $u$  decrease sharply near the loading surface and follow a little oscillatory pattern for all the four curves in the whole range of  $x$  with  $\Omega=0, 4$  and  $m=0.25, 0.5$  respectively. The variation of normal displacement with distance  $x$  has shown in Fig 7. It can be seen that its value reduces continuously in the range  $0 \leq x \leq 6$  for  $m=0.25$  and  $\Omega=0, 4$  respectively. Whereas for  $m=0.5$  and  $\Omega=4$  it decreases first in the range  $0 \leq x \leq 4$  then increases smoothly in the rest of the range and follow a little oscillatory pattern. Fig. 8 displays the change in the value of conductive temperature with distance  $x$ . we observed that it also follow the same pattern as in case of normal displacement i.e., firstly it decreases in the range  $0 \leq x \leq 4$  and increases in the whole range with increasing value of  $x$ . Fig. 9 and Fig. 10 gives the variation of tangential and normal stresses. It can be seen that the behavior is quite similar with the above discussed cases. It is observed that the variations for both follow a small oscillatory pattern with difference in the amplitude of oscillations.

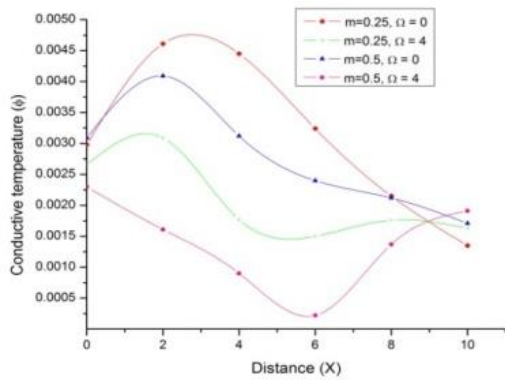


Fig. 13 Variation of conductive temperature  $\phi$  with distance  $x$  (linearly distributed mechanical force)

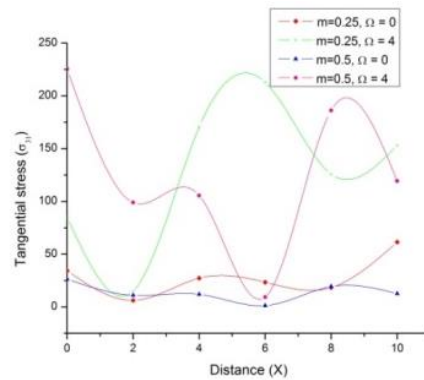


Fig. 14 Variation of tangential stress  $\sigma_{13}$  with distance  $x$  (linearly distributed mechanical force)

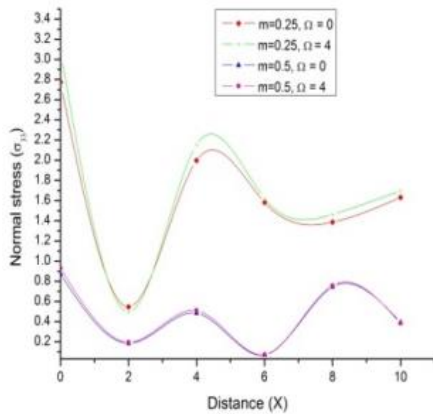


Fig. 15 Variation of normal stress  $\sigma_{33}$  with distance  $x$  (linearly distributed mechanical force)

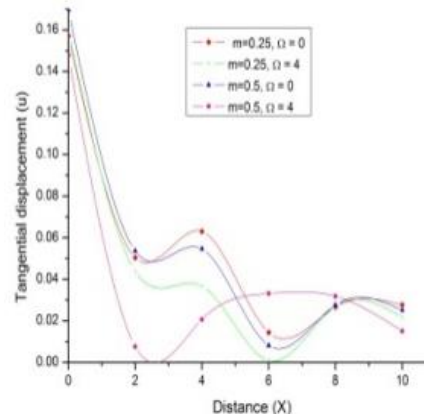


Fig. 16 Variation of displacement  $u$  with distance  $x$  (concentrated mechanical force)

## 10. Deformation due to mechanical force

### 10.1 Linearly distributed mechanical force

In linearly distributed mechanical force, Figs. 11-15 describes the effect of hall parameter on various components with and without rotation. Fig. 11 and Fig. 12 display the nature of displacements with distance  $x$  for two different values of hall parameter  $m=0.25, m=0.5$  and  $\Omega=0, 4$  respectively. In Fig. 11 it can be seen that for  $m=0.25$  and  $\Omega=0, 4$  in the beginning the value of displacement  $u$  decreases in the range  $0 \leq x \leq 4$  afterwards increases and shows an oscillatory behavior for the rest of the range. For  $m=0.5$  it also decreases in the beginning near the loading surface and follow an oscillatory pattern with small amplitude of oscillations with  $\Omega=0, 4$  respectively. Fig. 12 gives the behavior of normal displacement with distance  $x$ . We see that value of normal displacement varies in the same manner as the displacement  $u$  varies with little difference in the magnitude of oscillations and approaches to maximum value with increasing value of  $x$ . The variation of conductive temperature with distance  $x$  has shown in Fig. 13. It can be noticed that

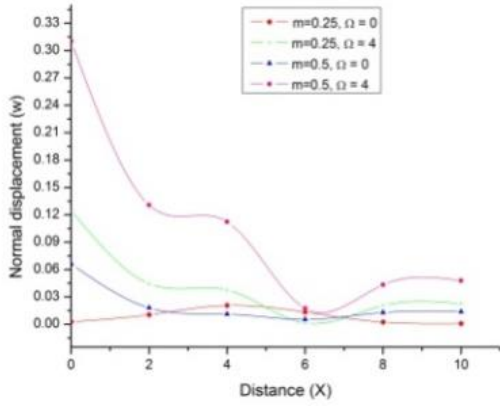


Fig. 17 Variation of normal displacement  $w$  with distance  $x$  (concentrated mechanical force)

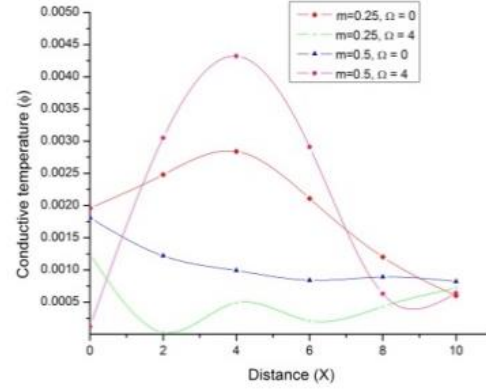


Fig. 18 Variation of conductive temperature  $\phi$  with distance  $x$  (concentrated mechanical force)

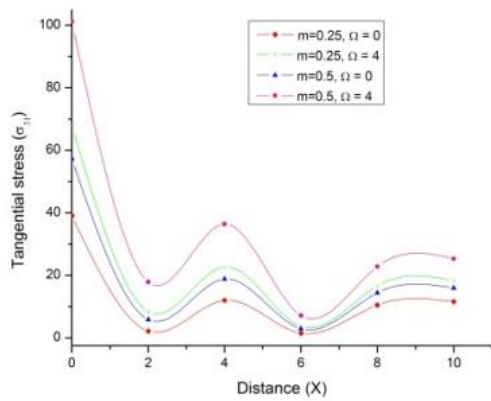


Fig. 19 Variation of tangential stress  $\sigma_{13}$  with distance  $x$  (concentrated mechanical force)

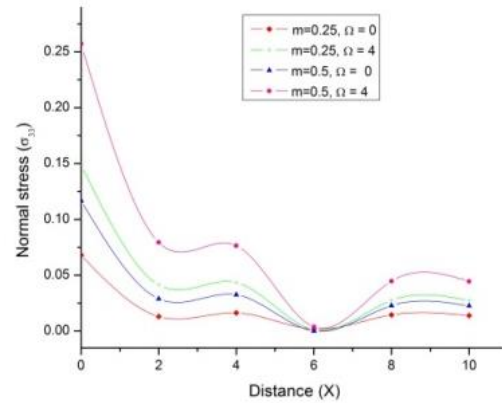


Fig. 20 Variation of normal stress  $\sigma_{33}$  with distance  $x$  (concentrated mechanical force)

for  $m=0.25$  and  $m=0.5$  with  $\Omega=0, 4$  the curve attains its maximum value in the beginning then suddenly falls down near  $x = 4$ , whereas for  $m=0.5$  and  $\Omega=4$  it decreases in the range  $2 \leq x \leq 4$  after that all the three curves begin to coincide when  $x$  approaches to its maximum value. Fig. 14 and Fig. 15 gives the variation of tangential and normal stresses with distance  $x$ . We observed that the distribution curves for both the stresses (tangential and normal) for  $m=0.25, m=0.5$  and  $\Omega=0, 4$  is oscillatory in nature with different amplitude of oscillations.

### 10.2 Concentrated mechanical force

Figs. 16-20 shows the characteristics for concentrated mechanical force. It is clear from the graphs that the distribution curves for displacement  $u$ , normal displacement  $w$ , conductive temperature  $\phi$ , tangential stress  $\sigma_{13}$  and normal stress  $\sigma_{33}$  follow the same trends as in case of concentrated thermal source for both values of hall parameter and rotation i.e.,  $m=0.25, m=0.5$  and  $\Omega=0, 4$  respectively.

## 11. Conclusions

In the present investigation, we have examined the effect of hall current on all the physical quantities with and without rotation in the presence of two temperature in generalized thermoelasticity. It is noticed that the hall current and rotation has a major impact on the stress components, displacement components and conductive temperature. We observed that the trends of all the components are almost oscillatory with difference in amplitude of oscillations. The magnitude of oscillations are either increasing or decreasing with increasing value of distance. In this problem we consider the heat conduction equation with refined multi-dual-phase-lags. Nowadays, this model is more appropriate to solve some practical problems of physical processes. The finding of this paper gives an inspiration to study about magneto-thermoelastic materials as an innovative domain of applicable thermoelastic solids. The results are also beneficial in real life problems and for their practical applications like in geophysics, geomagnetic etc. The validity of results is approved by comparing the temperature, displacements and stresses according to the present refined multi-phase-lag theory with those due to other thermoelasticity theories.

## References

- Abbas, I.A. (2014), "Nonlinear transient thermal stress analysis of thick-walled FGM cylinder with temperature-dependent material properties", *Meccanica*, **49**(7), 1697-1708. <http://doi.org/10.1007/s11012-014-9948-3>.
- Abbas, I.A. (2018a), "A study on fractional order theory in thermoelastic half-space under thermal loading", *Phys. Mesomech.*, **21**(2), 150-156. <http://doi.org/10.1134/S102995991802008X>.
- Abbas, I.A. (2018b), "Free vibrations of nanoscale beam under two-temperature Green and Naghdi Model", *Int. J. Acoust. Vib.*, **23**(3), 289-293. <http://doi.org/10.20855/ijav.2018.23.31051>.
- Abbas, I.A. and Youssef, H.M. (2009), "Finite element analysis of two-temperature generalized magneto thermoelasticity", *Arch. Appl. Mech.*, **79**(10), 917-925. <http://doi.org/10.1007/s00419-008-0259-9>.
- Abbas, I.A., Abd-alla, A.N. and Othman, M.I.A. (2011), "Generalized magneto-thermoelasticity in a fiber-reinforced anisotropic half-space", *Int. J. Thermophys.*, **32**(5), 1071-1085. <http://doi.org/10.1007/s10765-011-0957-3>.
- Abd-alla, A.N. and Abbas, I.A. (2002), "A problem of generalized magneto thermoelasticity for an infinitely long, perfectly conducting cylinder", *J. Therm. Stress.*, **25**(11), 1009-1025. <http://doi.org/10.1080/01495730290074612>.
- Abualnour, M., Chikh, A., Hebali, H., Kaci, A., Tounsi, A., Bousahla, A.A. and Tounsi, A. (2019), "Thermomechanical analysis of antisymmetric laminated reinforced composite plates using a new four variable trigonometric refined plate theory", *Comput. Concrete*, **24**(6), 489-498. <https://doi.org/10.12989/cac.2019.24.6.489>.
- Alzahrani, F.S. and Abbas, I.A. (2020), "Photo-thermal interactions in a semiconducting media with a spherical cavity under hyperbolic two-temperature model", *Math.*, **8**(585), 1-11. <http://doi.org/10.3390/math8040585>.
- Belbachir, N., Draich, K., Bousahla, A.A., Bourada, M., Tounsi, A. and Mohammadimehr, M. (2019), "Bending analysis of anti-symmetric cross-ply laminated plates under nonlinear thermal and mechanical loadings", *Steel Compos. Struct.*, **33**(1), 81-92. <https://doi.org/10.12989/scs.2019.33.1.081>.
- Bhatti, M.M., Ellahi, R., Zeeshan, A., Marin, M. and Ijaz, N. (2019), "Numerical study of heat transfer and Hall current impact on peristaltic propulsion of particle-fluid suspension with compliant wall properties", *Modern Phys. Lett. B*, **33**(35), 1950439. <http://doi.org/10.1142/S0217984919504396>.
- Biot, M.A. (1956), "Thermoelasticity and irreversible thermodynamics", *J. Appl. Phys.*, **27**(3), 240-253. <http://doi.org/10.1063/1.1722351>.

- Biswas, S. and Abo-Dahab, S.M. (2018), "Effect of phase lags on Rayleigh wave propagation in initially stressed magneto-thermoelastic orthotropic medium", *Appl. Math. Model.*, **59**, 713-727. <http://doi.org/10.1016/j.apm.2018.02.025>.
- Biswas, S., Mukhopadhyay, B. and Shaw, S. (2017a), "Thermal shock response in magneto-thermoelastic orthotropic medium with three-phase-lag model", *J. Electromagnet. Wave. Appl.*, **31**(9), 879-897. <http://doi.org/10.1080/09205071.2017.1326851>.
- Biswas, S., Mukhopadhyay, B. and Shaw, S. (2017b), "Rayleigh surface wave propagation in orthotropic thermoelastic solid under three phase lag model", *J. Therm. Stress.*, **40**(4), 403-419. <http://doi.org/10.1080/01495739.2017.1283971>.
- Bousahla, A.A., Bourada, F., Mahmoud, S.R., Tounsi, A., Algarni, A., Adda Bedia, E.A. and Tounsi, A. (2020), "Buckling and dynamic behavior of the simply supported CNT-RC beams using an integral-first shear deformation theory", *Comput. Concrete*, **25**(2), 155-166. <https://doi.org/10.12989/cac.2020.25.2.155>.
- Chen, P.J. and Gurtin, E.M. (1968), "On a theory of heat conduction involving two temperatures", *Zeitschrift für Angewandte Mathematik und Physik*, **19**(4), 614-627.
- Chen, P.J., Gurtin, M.E. and Williams, O.W. (1969), "On the thermodynamics of non-simple elastic materials with two temperatures", *Zeitschrift für Angewandte Mathematik und Physik*, **20**(1), 107-112.
- Chen, P.J., Gurtin, M.E. and Williams, W.O. (1968), "A note on non-simple heat conduction", *Zeitschrift für Angewandte Mathematik und Physik ZAMP*, **19**(4), 969-970.
- Chikr, S.C., Kaci, A., Bousahla, A.A., Bourada, F., Tounsi, A., Adda Bedia, E.A., Mahmoud, S.R., Benrahou, S.R. and Tounsi, A. (2020), "A novel four-unknown integral model for buckling response of FG sandwich plates resting on elastic foundations under various boundary conditions using Galerkin's approach", *Geomech. Eng.*, **21**(5), 471-487. <https://doi.org/10.12989/gae.2020.21.5.471>.
- Das, B. and Lahiri, A. (2015), "Generalized Magneto-thermoelasticity for isotropic media", *J. Therm. Stress.*, **38**(2), 210-228. <http://doi.org/10.1080/01495739.2014.985564>.
- Draiche, K., Bousahla, A.A., Tounsi, A., Alwabli, A.S., Tounsi, A. and Mahmoud, S.R. (2019), "Static analysis of laminated reinforced composite plates using a simple first order shear deformation theory", *Comput. Concrete*, **24**(4), 369-378. <https://doi.org/10.12989/cac.2019.24.4.369>.
- Ezzat, M.A., EL-Karamany, A.S. and EL-Bary, A.A. (2014), "Magneto-thermoelasticity with two fractional order heat transfer", *J. Assoc. Arab Univ. Basic Appl. Sci.*, **19**, 70-79. <http://doi.org/10.1016/j.jau.bas.2014.06.009>.
- Honig, G. and Hirdes, U. (1984), "A method for numerical inversion of Laplace transforms", *J. Comput. Appl. Math.*, **10**(1), 113-132. [http://doi.org/10.1016/0377-0427\(84\)90075-x](http://doi.org/10.1016/0377-0427(84)90075-x).
- Kaddari, M., Kaci, A., Bousahla, A.A., Tounsi, A., Bourada, F., Tounsi, A., Adda Bedia, E.A. and Al-Osta, M.A. (2020), "A study on the structural behaviour of functionally graded porous plates on elastic foundation using a new quasi-3D model: Bending and Free vibration analysis", *Comput. Concrete*, **25**(1), 37-57. <https://doi.org/10.12989/cac.2020.25.1.037>.
- Kumar, R. and Abbas, I.A. (2013), "Deformation due to thermal source in micropolar thermoelastic media with thermal and conductive temperatures", *J. Comput. Theor. Nanosci.*, **10**(9), 2241-2247. <http://doi.org/10.1166/jctn.2013.3193>.
- Kumar, R. and Chawla, V. (2014), "General solution and fundamental solution for two-dimensional problem in orthotropic thermoelastic media with voids", *J. Adv. Math. Appl.*, **3**(1), 47-54. <http://doi.org/10.2298/TAM1404247>.
- Kumar, R., Sharma, N. and Lata, P. (2016), "Thermomechanical interactions in transversely isotropic magneto-thermoelastic medium with vacuum and with and without energy dissipation with combined effects of rotation, vacuum and two temperatures", *Appl. Math. Model.*, **40**(13-14), 6560-6575. <http://doi.org/10.1016/j.apm.2016.01.061>.
- Kumar, R., Sharma, N. and Lata, P. (2016), "Thermomechanical interactions due to hall current in transversely isotropic thermoelastic with and without energy dissipation with two temperatures and rotation", *J. Solid Mech.*, **8**(4), 840-858.
- Kumar, R., Sharma, N. and Lata, P. (2017a), "Effects of hall current and two temperature transversely isotropic magneto-thermoelastic with and without energy dissipation due to ramp type heat", *Mech. Adv. Mater.*

- Struct.*, **24**(8), 625-635. <http://doi.org/10.1080/15376494.2016.1196769>.
- Kumar, R., Sharma, N., Lata, P. and Abo-Dahab, S.M. (2017b), "Rayleigh waves in anisotropic magneto thermoelastic medium", *Coupl. Syst. Mech.*, **6**(3), 317-333. <http://doi.org/10.12989/csm.2017.6.3.317>.
- Lata, P. (2018), "Effect of energy dissipation on plane waves in sandwiched layered thermoelastic medium", *Steel Compos. Struct.*, **27**(4), 439-451. <http://doi.org/10.12989/scs.2018.27.4.439>.
- Lata, P. and Kaur, I. (2018), "Effect of hall current in transversely isotropic magneto-thermoelastic rotating medium with fractional order heat transfer due to normal force", *Adv. Mater. Res.*, **7**(3), 203-220. <http://doi.org/10.12989/amr.2018.7.3.203>.
- Lata, P. and Kaur, I. (2019a), "Transversely isotropic magneto thermoelastic solid with two temperature and without energy dissipation in generalized thermoelasticity due to inclined load", *SN Appl. Sci.*, **1**(5), 1-13. <http://doi.org/10.1007/s42452-019-0438-z>.
- Lata, P. and Kaur, I. (2019b), "Effect of hall current on a propagation of plane wave in transversely isotropic thermoelastic medium with two temperature and fractional order heat transfer", *SN Appl. Sci.*, **1**(8), 1-16. <http://doi.org/10.1007/s42452-019-0942-1>.
- Lata, P. and Kaur, I. (2019c), "Effect of rotation and inclined load on transversely isotropic magneto thermoelastic solid", *Struct. Eng. Mech.*, **70**(2), 245-255. <http://doi.org/10.12289/sem.2019.70.2.245>.
- Lata, P. and Kaur, I. (2020), "Thermomechanical interactions in transversely isotropic magneto-thermoelastic medium with fractional order generalized heat transfer and hall current", *Arab J. Basic Appl. Sci.*, **27**(1), 13-26. <https://doi.org/10.1080/25765299.2019.1703494>.
- Lata, P. and Zakhmi, H. (2019), "Fractional order generalized thermoelastic study in orthotropic medium of type GN-III", *Geomech. Eng.*, **19**(4), 295-305. <http://doi.org/10.12989/gae.2019.19.4.295>.
- Lata, P. and Zakhmi, H. (2020), "Time harmonic interactions in an orthotropic media in the context of fractional order theory of thermoelasticity", *Struct. Eng. Mech.*, **73**(6), 725-735. <http://doi.org/10.12989/sem.2020.73.6.725>.
- Lord, H.W. and Shulman, Y. (1967), "A generalized dynamical theory of thermoelasticity", *J. Mech. Phys. Solid.*, **15**, 299-309. [http://doi.org/10.1016/0022-5096\(67\)90024-5](http://doi.org/10.1016/0022-5096(67)90024-5).
- Marin, M. (1994), "The Lagrange identity method in thermoelasticity of bodies with microstructure", *Int. J. Eng. Sci.*, **32**(8), 1229-1240. [http://doi.org/10.1016/0020-7225\(94\)90034-5](http://doi.org/10.1016/0020-7225(94)90034-5).
- Marin, M. (1995), "On existence and uniqueness in thermoelasticity of micropolar bodies", *Comptes Rendus De L'Academie Des Sciences Serie II Fascicule B-Mecanique Physique Astronomie*, **321**(12), 475-480.
- Marin, M. (2010), "Some estimates on vibrations in thermoelasticity of dipolar bodies", *J. Vib. Control*, **16**(1), 33-47. <http://doi.org/10.1177/1077546309103419>.
- Marin, M. (1997), "An uniqueness result for body with voids in linear thermoelasticity", *Rendiconti di Matematica*, **17**(7), 103-113.
- Marin, M., Craciun, E.M. and Pop, N. (2016), "Considerations on mixed initial-boundary value problems for micropolar porous bodies", *Dyn. Syst. Appl.*, **25**(1-2), 175-196.
- Matouk, H., Bousahla, A.A., Heireche, H., Bourada, F., Adda Bedia, E.A., Tounsi, A., Mahmoud, S.R., Tounsi, A. and Benrahou, K.H. (2020), "Investigation on hygro-thermal vibration of P-FG and symmetric S-FG nanobeam using integral Timoshenko beam theory", *Adv. Nano Res.*, **8**(4), 293-305. <https://doi.org/10.12989/anr.2020.8.4.293>.
- Othman, M.I.A. and Abbas, I.A. (2011), "Effect of rotation on plane waves at the free surface of a fiber reinforced thermoelastic half-space using the finite element method", *Meccanica*, **46**(2), 413-421. <http://doi.org/10.1007/s11012-010-9322-z>.
- Press, W.H., Teukolsky, S.A., Vetterling, W.T. and Flannery, B.P. (1986), *FORTRAN Numerical Recipes*, Cambridge University Press Cambridge.
- Rahmani, M.C., Kaci, A., Bousahla, A.A., Bourada, F., Tounsi, A., Adda Bedia, E.A., Mahmoud, S.R., Benrahou K.H. and Tounsi A. (2020), "Influence of boundary conditions on the bending and free vibration behavior of FGM sandwich plates using a four-unknown refined integral plate theory", *Comput. Concrete*, **25**(3), 225-244. <https://doi.org/10.12989/cac.2020.25.3.225>.
- Refrati, S., Bousahla, A.A., Bouhadra, A., Menasria, A., Bourada, F., Tounsi, A., Adda Bedia, E.A., Mahmoud, S.R., Benrahou, K.H. and Tounsi, A. (2020), "Effects of hygro-thermo-mechanical conditions on the

- buckling of FG sandwich plates resting on elastic foundations”, *Comput. Concrete*, **25**(4), 311-325. <https://doi.org/10.12989/cac.2020.25.4.311>.
- Riaz, A., Ellahi, R., Bhatti, M.M. and Marin, M. (2019), “Study of heat and mass transfer in the Eyring-Powell model of fluid propagating peristaltically through a rectangular compliant channel”, *Heat Transf. Res.*, **50**(16), 1539-1560. <http://doi.org/10.1615/HeattransRes.2019025622>.
- Schoenberg, M. and Censor, D. (1973), “Elastic waves in rotating media”, *Quart. Appl. Math.*, **31**, 115-125. <http://doi.org/10.1090/QAM/99708>.
- Sharma, K. and Marin, M. (2014), “Reflection and transmission of waves from imperfect boundary between two heat conducting micropolar thermoelastic solids”, *Analele Universitatii “Ovidius” Constanta-Seria Mathematica*, **22**(2), 151-175. <http://doi.org/10.2478/auom-2014-0040>.
- Sharma, N., Kumar, R. and Lata, P. (2015), “Disturbance due to inclined load in transversely isotropic thermoelastic medium with two temperatures and without energy dissipation”, *Mater. Phys. Mech.*, **22**(2), 107-117.
- Tounsi, A., Al-Dulaijan, S.U., Al-Osta, M.A., Chikh, A., Al-Zahrani, M.M., Sharif, A. and Tounsi, A. (2020), “A four variable trigonometric integral plate theory for hygro-thermo-mechanical bending analysis of AFG ceramic-metal plates resting on a two-parameter elastic foundation”, *Steel Compos. Struct.*, **34**(4), 511-524. <https://doi.org/10.12989/scs.2020.34.4.51>.
- Tzou, D.Y. (1995), “A unified field approach for heat conduction from macro to micro scales”, *ASME J. Heat Transf.*, **117**(1), 8-16. <https://doi.org/10.1115/1.2822329>.
- Youssef, H.M. (2006), “Theory of two temperature generalized thermoelasticity”, *IMA J. Appl. Math.*, **71**(3), 383-390. <http://doi.org/10.1093/imamat/hxh101>.
- Zakaria, M. (2012). “Effects of hall current and rotation on magneto-micropolar generalized thermoelasticity due to ramp-type heating”, *Int. J. Electromagnet Appl.*, **2**(3), 24-32. <http://doi.org/10.5923/j.ijea.20120203.02>.
- Zenkour, A.M. (2020), “Magneto-thermal shock for a fiber-reinforced anisotropic half-space studied with a refined multi-dual-phase-lag model”, *J. Phys. Chem. Solid.*, **137**, <https://doi.org/10.1016/j.jpcs.2019.109213>.